INDC 416

International Atomic Energy Agency

INDC(URU)-1/G

INDC INTERNATIONAL NUCLEAR DATA COMMITTEE

PROGRESS REPORT FROM URUGUAY TO THE INDC

Submitted by N. Azziz

June 1971

IAEA NUCLEAR DATA SECTION, KÄRNTNER RING 11, A-1010 VIENNA

NEUTRON CROSS SECTIONS WITH SINGLE AND DOUBLE PARTICLE EMISSION

N. AZZIZ - E. HORJALES

Dpto.de Fisica Nuclear.

INSTITUTO DE FISICA

Abstract:

The cross sections (n, n), (n, 2n), (n, α), (n, α n), (n, nα), (n,p) etc., for energies in the MeV region, were predicted using an statistical model and no normalization factor was needed. As an application Cu^{65} was taken as a target. The experimental and theoretical predictions show satisfactory agreement.

I) Introduction:

The nuclear density formula derived by Gilbert and Cameron has been modified at low energy and applied to calculate fast neutron cross sections using the nuclear statistical model. This very simple picture of the nucleus used carefully reproduces the experimental data satisfactorily. Contrary to most calculations, no normalization factor was used and satisfactcry agreement with the experiment was obtained.

The capture cross sections, necessary for the calculations, were obtained from experiment, when available, or theoretical calculations which were based on an optical potential model for the nucleus.

The code called Reduce and written for this purpose will be available at Argonne National Center Code Distribution.

II) Theory:

As is well known, the statistical model of the nucleus is based in the compound nucleus theory of Bohr and on the time reverse invariance of the nuclear reactions. This model is an oversimplification of the actual complex phenomena that occur during a nuclear reaction. However, in certain neutron energy range this is the only model which allows a reasonable mathematical treatment of the problem. The future closed shell and pairing effects of the nucleus, which we know are important, were included into the model throughout the nuclear temperature parameter.

Two or more particle emission:

Suppose we are dealing with a reaction where α is the incoming particle, and β, δ and ε are emitted in a successive manner passing through different residual nuclei.

Diagrammatically this looks like,

$$A + \alpha \longrightarrow \begin{array}{l} B^* + \beta \\ \downarrow \\ C^* + \delta \\ \downarrow \\ D^* + \varepsilon \end{array}$$

During this first step we may assume with N. Bohr that the cross section of β emission is given by

$$\sigma(\alpha,\beta) = \sigma(\alpha)\,\frac{\Gamma(\beta)}{\Gamma(c)} \qquad (1)$$

where $\sigma(\alpha)$ is the capture cross section of α by A, $\Gamma(\beta)$ the probability of emission of β and $\Gamma(c)$ the total probability of emission of β and any other particle,

$$\Gamma(c) = \sum_i \Gamma(i)$$

similarly for two particle emission,

$$\sigma(\alpha,\beta,\delta) = \sigma(\alpha)\,\frac{\Gamma(\beta,\delta)}{\Gamma(c)} \qquad (2)$$

where $\Gamma(\beta\delta)$ is the compound probability of β and δ emission in a successive manner.

Accordingly, to the time reverse invariance of the nuclear reactions, for the one particle emission the following relationship holds

$$k_\alpha^2\,\Gamma(\beta)\sigma(\alpha) = k_\beta^2\,\Gamma(\alpha)\sigma(\beta)$$

By this relationship (1) may be written as

$$\sigma(\alpha,\beta) = \sigma(\alpha)\left[k_\beta^2\,\sigma(\beta)\Big/\sum_i k_i^2\,\sigma(i)\right] \qquad (3)$$

If the particle β may be released with a spectrum of energy, then the probability $k_\beta^2\sigma(\beta)$ for emission of a particle β is replaced by the integral $\Gamma(\beta)$

$$\Gamma(\beta) = \frac{g_\beta}{2\pi^2\rho_c(v_c)} \int_0^{E_\beta^{max}} dE_\beta\, k_\beta^2\,\sigma(\beta)\,\rho_\beta(v_\beta) \qquad (4)$$

The statistical weighting factor g_β is equal to $(2S_\beta + 1)$ for a particle whose spin is S_β. If the emitted object is a gamma ray, then $g_\beta k_\beta^2$ is replaced by $(2E_\beta/c)^2$, C is the speed of light and E_β the energy of the gamma ray. The quantities $\rho_c(v_c)$ and $\rho_\beta(v_\beta)$ are

the nuclear densities of the nuclear densities of the nuclei $(A + \alpha)$ and B at the excitation energies υ_c and υ_B respectively. Theoretically the capture cross section $\sigma(\beta)$ should be calculated at the excitation energy υ, however, in practice it is done with the nucleus B in its ground state.

In analogous way to equation (4) the compound probability $\Gamma(\beta\delta)$ may be written as

$$\Gamma(\beta\delta) = \frac{g_B}{2\pi^2 \rho_A(\upsilon_A)} \int_0^{E_\beta^{max}} dE_\beta \, k_\beta^2 \, \sigma(\beta) \, \rho_B(\upsilon_B) \, P_{\beta\delta}$$

where the probability $P_{\beta\delta}$ is given by

$$P_{\beta\delta} = \frac{R_{\beta\delta}}{\sum_i' R_{\beta i}}$$

where

$$R_{\beta i} = \frac{g_i}{2\pi^2 \rho_\beta(\upsilon_B)} \int_0^{E_i^{max}} dE_i \, k_i^2 \, \sigma(i) \, \rho_c(\upsilon_c)$$

The maximum energy of the emitted particle i E_i^{max} is related to the energy of the β particle (see figure 1) by

$$E_i^{max} = E_\beta^{max} + Q_{BC} - E_\beta$$

where

$$E_\beta^{max} = E_\kappa + Q_{AB}$$

The residual nucleus after the emission of particle i is $C = A + \alpha$
The Q values for the reaction $A(\alpha, \gamma)(A+\alpha)$, $A(\alpha, \beta)B$ and $B(\gamma, i)C$ are indicated by $Q^A_{\alpha\beta}$, Q_{AB}, Q_{BC}

The excitation energies υ are given by

$$\upsilon_A = E + Q^A_{\alpha\gamma}$$

$$\upsilon_B = E_\beta^{max} - E_\beta$$

and

$$\upsilon_c = E_i^{max} - E_i$$

It should be pointed out that we denominate $\sigma(\alpha,\beta)$ the cross section which is free of contributions from any other particle emission. That is, after β is emitted, the nucleus B is left in its ground state or in an excited state that may only decay by γ emission,

$$\sigma(\alpha,\beta) = \sigma^*(\alpha,\beta) - \sum_{\delta \neq \gamma} \sigma(\alpha,\beta,\delta)$$

where $\sigma^*(\alpha,\beta)$ is determined by (3) and (4).

III. Nuclear Density:

We have used the nuclear density given by Gilbert and Cameron[1]

$$\rho(U,J) = \frac{1.11}{A} \frac{\exp(2\sqrt{aU})}{a U^2} (2J+1) \exp\left[-(J+\tfrac{1}{2})^2/2\sigma^2\right] \qquad (5)$$

where

$$\sigma^2 = 0.0888\, A^{2/3} \sqrt{aU}$$

The observable density is given by the sum of $\rho(U,J)$ over all possible J values.
In absence of other information this summation is replaced by an integral in J from zero to infinity. The result is

$$\rho(U) = \frac{0.2}{A^{1/3}} \frac{\exp(2\sqrt{aU})}{a^{1/2} U^{3/2}} \qquad (6)$$

The parameter a is according to Bethe proportional to the mass number A. Gilbert and Cameron have included the shell correction S in the expression of a. Since the nuclear density is deduced assuming that the nucleus is a Fermi sea without surface effect or any nuclear interaction, shell and pairing effect should be included in a semi-empirical fashion.

Thus they proposed to write

$$a/A = \alpha S + \beta$$

where α and β are constant to be determined from experiment. The pairing effect is taken into account by reducing the excitation energy by the amount δ_o. This means that δ_o must be expended before the system can be considered as formed by independent nucleons.

Below we explain how the density at low energy was alleviated. In this regard we point out that in spite of it is meaningless to talk about nuclear density at low energy, the numerical calculations depend quite critically on its value. We have taken a simple expression of ρ similar to (6) but the value of δ_o, the pairing parameter, was modified.

For odd-even and even-even nuclei δ_o was reduced with respect to its value at high energies. For odd-odd, δ_o being zero, the desired effect was obtained by creating a negative pairing effect.

In summary

$$\delta = \delta_o \left(1 - \frac{6-U}{12}\right) \qquad \text{for even-even,} \quad U < 6 \text{ MeV}$$

$$\delta = \delta_o \left(1 - \frac{6-U}{6}\right) \qquad \text{for odd-even,} \quad U < 6 \text{ MeV}$$

$$\delta = \frac{5-U}{6} \qquad \text{for odd-odd and} \quad U < 5 \text{ MeV}$$

Using this simple criterion, a remarkable agreement of the modified ρ at low energy and the temperature model $\exp[(U-E_o)/T]$ whose parameters E_o and T are reported by Gilbert and Cameron, was found. Besides the continuity of ρ between low and high energy is automatically obtained because the same analytic form (6) is used for both regions. Finally at very low energy $U < 0.2$ MeV was assumed to an exponential function joining smoothly ρ for $U \geq 0.2$ MeV. The procedure described here gives very good agreement with the observable level separation distance.

IV. Capture Cross Sections

The neutron capture cross section is quite known experimentally. However, the α, p, and γ capture are not so well known and we have used theoretical models for their prediction. The α capture cross section was obtained using the model of Hizenga and Igo. This model uses an optical model given by

$$V(r) = (V_o + iW_o) \Big/ \left[1 + \exp \frac{r-R}{a}\right]$$

where $V_o = -50$ MeV, $R = 1.17\,A + 1.77$, $a = 0.576$ and W ranges between 5 and 30 MeV. The coulomb potential used in this model is the one proposed by Hill and Ford[3]

$$V_c = \frac{2Ze^2}{R_c}\left[\frac{1}{\eta^2} + \frac{1}{2} - \frac{1}{6}x^2 + \frac{e^{-\eta}}{\eta^2}\left(\frac{1-e^{\eta x}}{\eta x} + \frac{1}{2}e^{\eta x}\right)\right] \Big/ \left(\frac{1}{3} + \frac{2}{\eta^2} + \frac{e^{-\eta}}{\eta^3}\right) \qquad \text{for } x < 1$$

$$V_c = \frac{2Ze^2}{R_c}\left[\frac{1}{x} - \left(\frac{(1/x + \eta/2)\, e^{\eta - \eta x}}{e^{-\eta} + 2\eta + \frac{1}{3}\eta^3}\right)\right] \qquad \text{for } x > 1$$

where $x = \frac{r}{R_c}$ and $R_c = 1.17\ A^{1/3}$

The value of n is 10 for heavy elements and is in general, proportional to $A^{1/3}$.

To calculate the proton capture cross sections, an optical model with the following parameters is used.

$$V_{opt}(r) = V_{re}(r) + iV_{im}(r) + \left(\frac{\hbar}{m_\pi c}\right)^2 V_{so}\ \frac{1}{r}\left[\frac{d}{dr}\left(V_{re}(r)\right)\right] \bar{l} \cdot \bar{\sigma}$$

where,

$$V_{re}(r) = \frac{V_0}{1 + \exp\left[(r - R_1)/a\right]}$$

$$V_{im}(r) = \frac{W_0}{1 + \exp\left[(r - R_2)/b\right]}$$

$$V_{so} = 5.5\ \text{MeV}\ ,\quad R_1 = R_2 = 1.25\ A^{1/3}\ \text{fm}$$

and $a = 0.65$ fm , $b = 0.90$ fm

The depth V_0 of the real part was calculated from the formula

$$V_0 = -48.6 + 0.3\,(E - \bar{V}_c) - 30\,\frac{N-Z}{A} \quad \text{MeV}$$

deduced from a microscopic many-body theory[4]

The last term is equivalent to the symmetry term in the semi-empirical mass formula.

The incoming proton energy is indicated by E and $\bar{V}_c$ represents the effect of the slowing down of the proton in nuclear matter due to the Coulomb effect.

If we include a diffusivity effect on the Coulomb distribution, V_c becomes

$$V_c = \frac{6}{5} \cdot \frac{Z e^2}{R}\,(1 - d) \quad \text{MeV}$$

The factor (1-d) is of the order of 0.65 for medium and heavy elements. The γ capture cross section was predicted using the formula proposed by Brink. This formula accounts for the giant dipole resonance with the empirical value of the resonance energy

$$E_R = 80\ A^{-1/3} \quad \text{MeV}$$

and a width $\Gamma_R = 5$ MeV. The formula is a classical Lorentizian distribution and reads:

$$\sigma_\gamma = \left[\frac{0.013\,A}{\Gamma_R}(\text{MeV})\right]\frac{E^2\,\Gamma_R^2}{(E^2-E_R^2)+E^2\,\Gamma_R^2} \quad \text{barns}$$

V. Results and Conclusions

In Figs. 4 to 11 we show our theoretical predictions by solid curves. The experimental ones, when available, are indicated in the same figures by arrows. Shaded areas represent the dispersion of such experimental data.

The experimental sources for the capture cross sections were taken from BNL 325. In the calculation of certain cross sections as (n,p) the capture cross section in the inverse reaction, plays an important role. For energies less than 4 MeV close to the threshold, the optical model used to calculate the p capture was not very adequate. In that case we took, for energies less than 4 MeV the experimental capture cross sections given in reference 6.

The experimental values of the one and two particle emission used to amke the comparison with the theoretical predictions, were taken from BNL 325.

As a conclusion we may say that in spite of the simplicity of the model, when it is worked out carefully, it becomes a powerful tool for the predictions of fast neutron cross sections.

REFERENCES

1) A. Gilbert and A.G.W. Cameron-Canadian Journal of Physics 43, 1446

2) J.R. Huizenga and G. Igo - Nuclear Physics 29, p. 462, 1962

3) K.W. Ford and D.L. Hill - Physical Review 94, p. 1617, 1954

4) N. Azziz - Nuclear Physics, A 141 (1970), 401

5) D.M. Brink - Thesis, Oxford University, 1955

6) F.K. Mc.Gowan, W.T. Milner and H.J. Kim - Nuclear cross sections for charged-particle induced reactions. Ni, Cu. ORNL-CPX-2

Figure Captions

Fig. 1 Neutron capture cross section for Cu^{65}. The $\overline{\sigma_c}$ for the other isotopes were found to be quite close (in a 5%) to this one.

Fig. 2 Alpha capture cross section for Co^{62}. Obtained from calculations with an optical model as explained in section IV.

Fig. 3 Proton capture cross section for Ni^{65}, obtained from calculations and experiment as explained in sections IV and V.

Fig. 4 Cu^{65} (n,n') Cu^{65} reaction cross section. The solid curve represents the theoretical predictions.

Fig. 5 Cu^{65} (n,α) Co^{62} reaction cross section. The solid curve represents the theoretical predictions.

Fig. 6 Cu^{65} (n,p) Ni^{65} reaction cross section. The solid curve represents the theoretical predictions. The dispersion of the experimental data is indicated with a shaded area.

Fig. 7 Cu^{65} (n,γ) Cu^{66} reaction cross section. The solid curve represents the theoretical predictions. The dispersion of the experimental data is indicated with a shaded area.

Fig. 8 Cu^{65} (n, 2n) Cu^{64} reaction cross section. The solid curve represents the theoretical predictions. The dispersion of the experimental data is indicated with a shade area.

Fig. 9 Cu^{65} (n, np) Ni^{64} and Cu^{65} (n,pn) Ni^{64} reaction cross sections. The solid curve represents the theoretical predictions.

Fig. 10 Cu^{65} (n, nα) Co^{61} reaction cross section. The solid curve represents the theoretical predictions. The dispersion of the experimental data is indicated with a shade area.

Fig. 11 Cu^{65} (n, α n) Co^{61} reaction cross section. The solid curve represents the theoretical predictions.

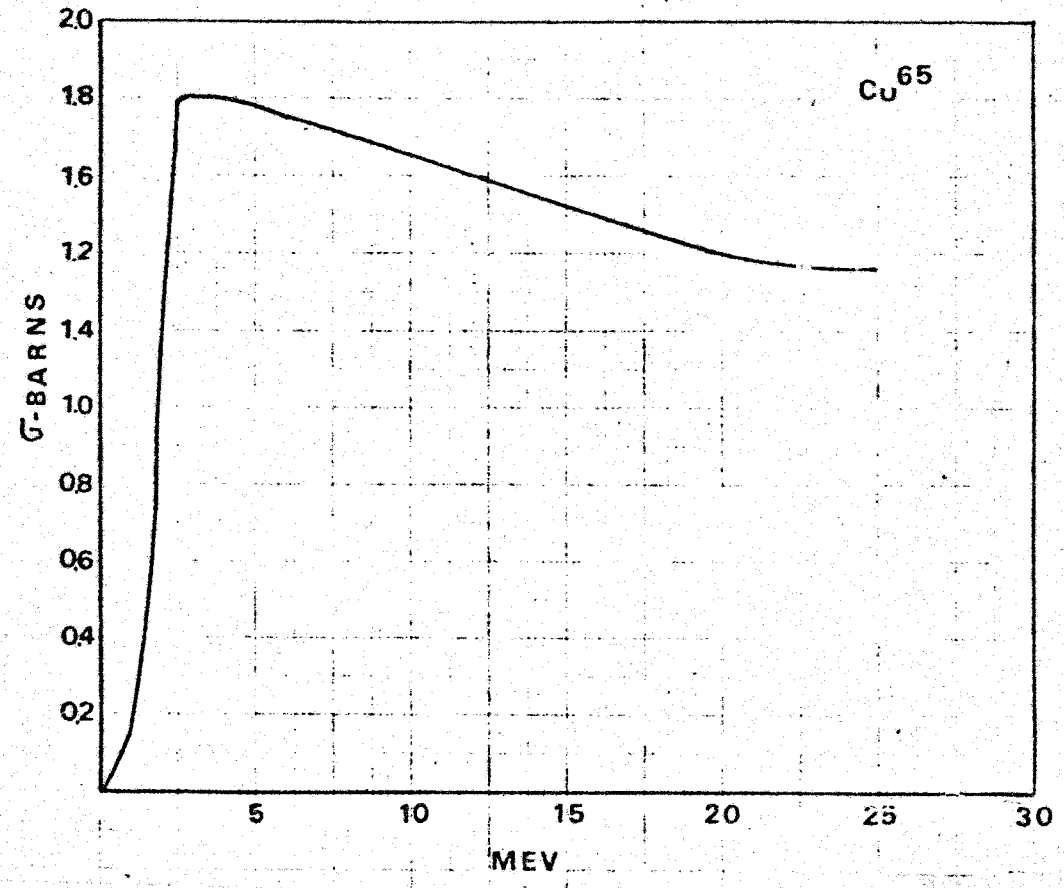
2.0
1.8
1.6
1.2
1.4
1.0
0.8
0.6
0.4
0.2
G-BARNS
Cu^{65}
5
10
15
20
25
30
MEV

Fig. 1

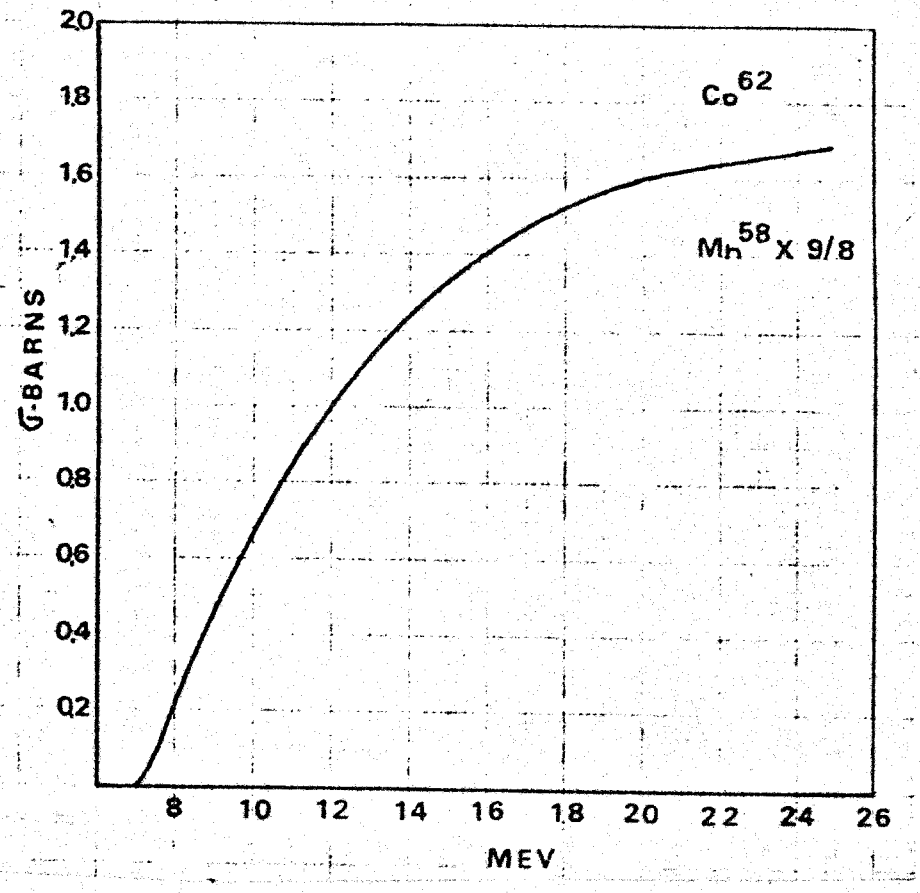
2.0
1.8
1.6
1.4
1.2
1.0
0.8
0.6
0.4
0.2
G-BARNS
Co^{62}
Mn^{58} X 9/8
8
10
12
14
16
18
20
22
24
26
MEV

Fig. 2

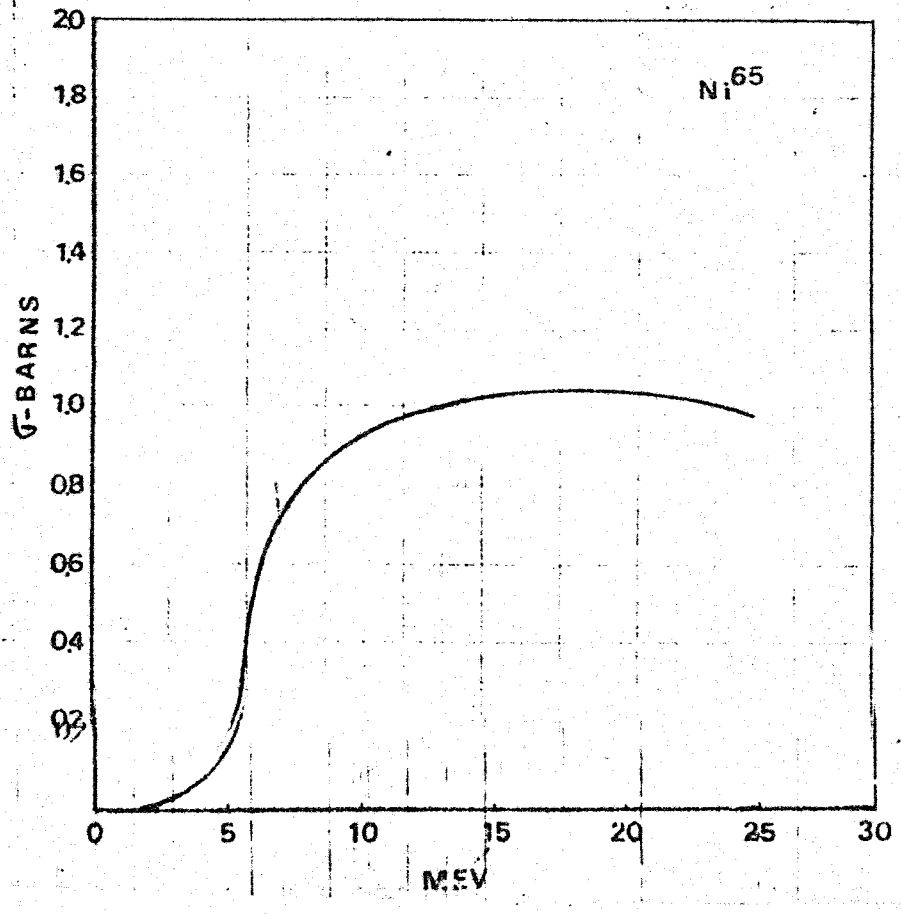
Ni65
σ-BARNS
2.0
1.8
1.6
1.4
1.2
1.0
0.8
0.6
0.4
0.2
0
5
10
15
20
25
30
MEV

Fig. 3

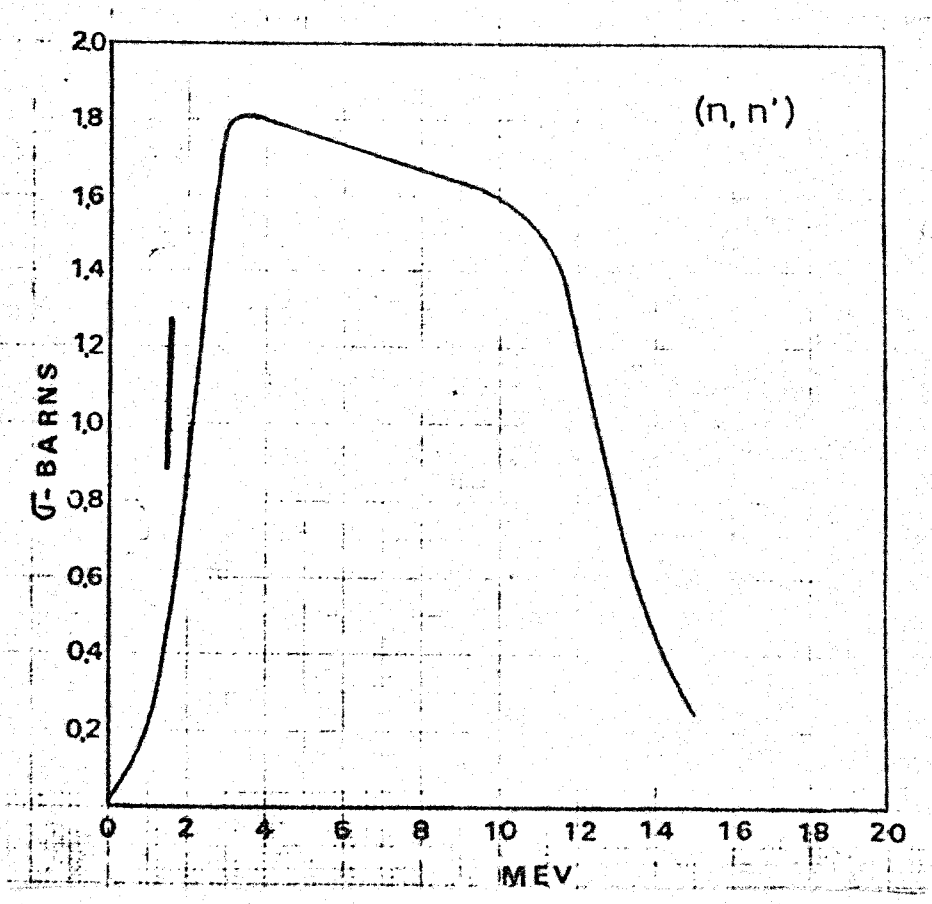
(n, n')
σ-BARNS
2.0
1.8
1.6
1.4
1.2
1.0
0.8
0.6
0.4
0.2
0
2
4
6
8
10
12
14
16
18
20
MEV

Fig. 4

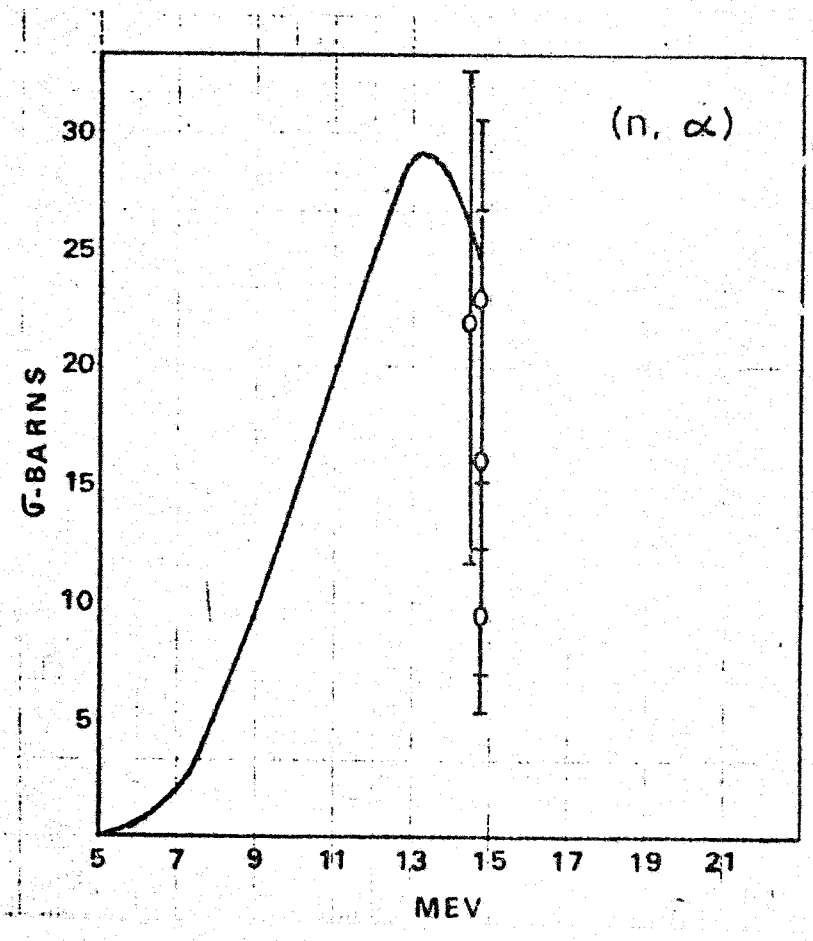
(n, α)
30
25
20
15
10
5
σ-BARNS
5
7
9
11
13
15
17
19
21
MEV

Fig. 5

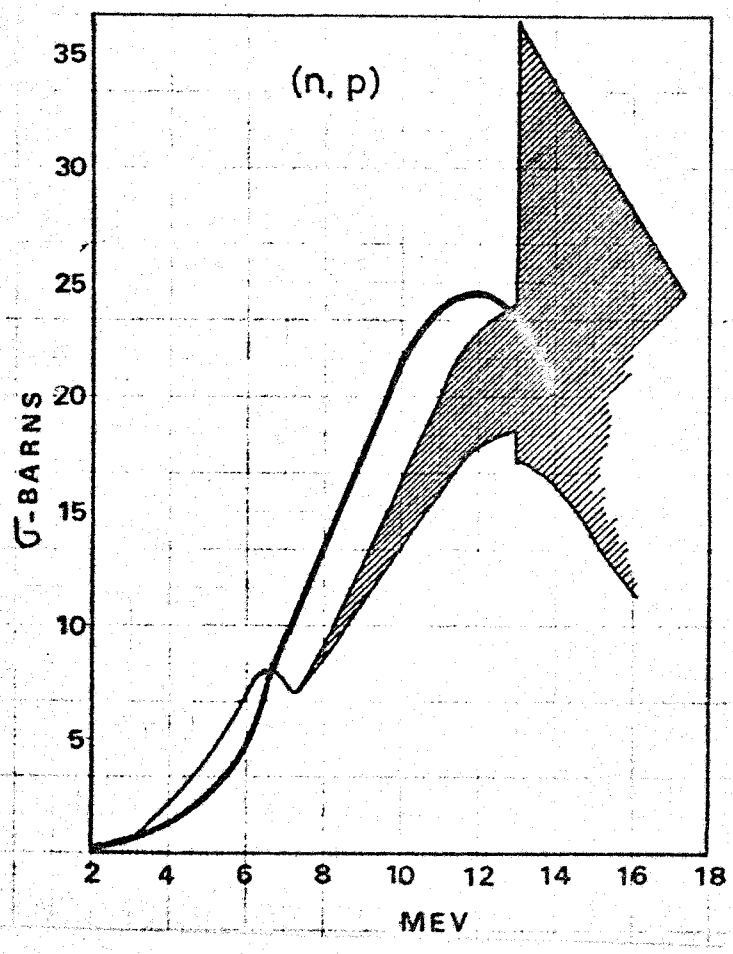
(n, p)
35
30
25
20
15
10
5
σ-BARNS
2
4
6
8
10
12
14
16
18
MEV

Fig. 6

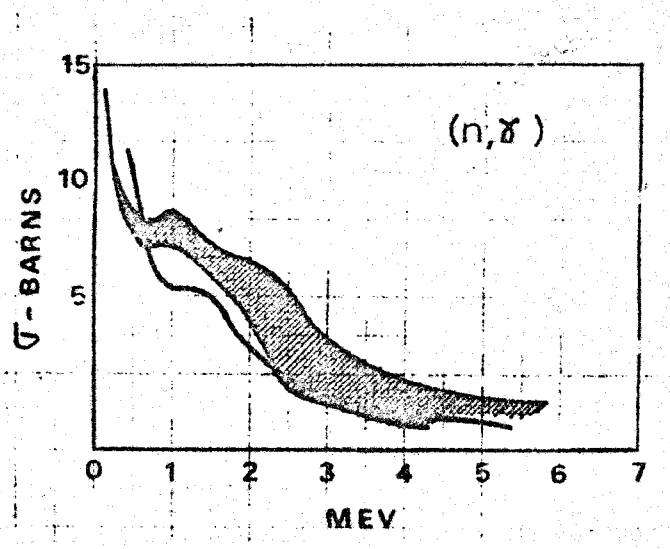

Fig. 7

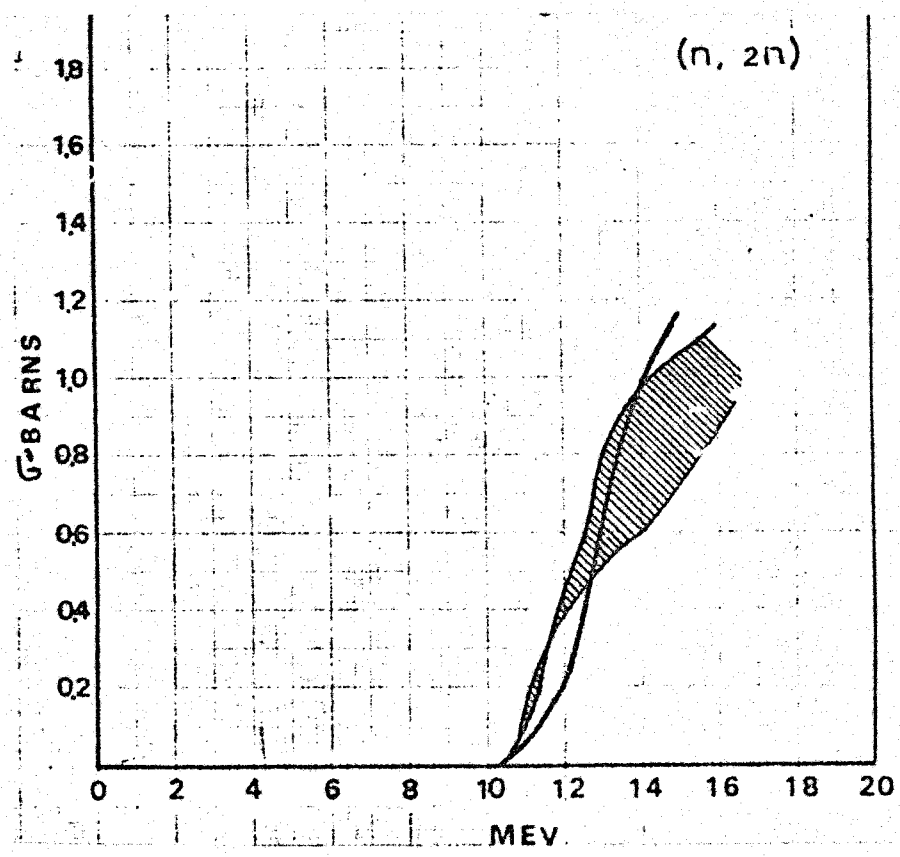

Fig. 8

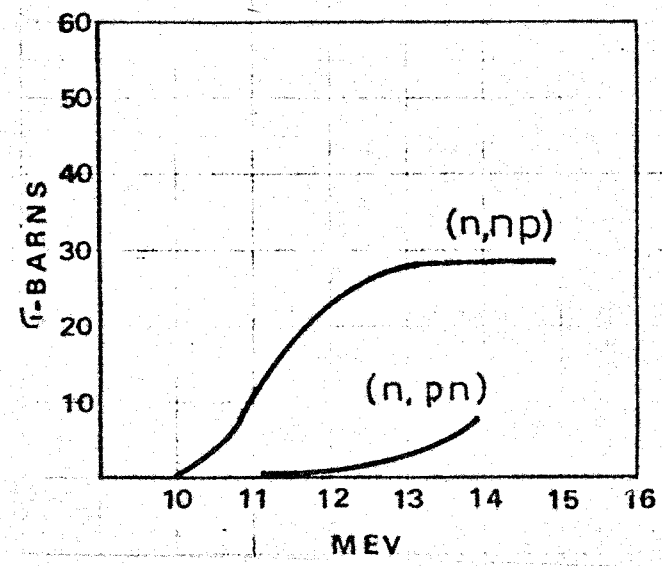

Fig. 9

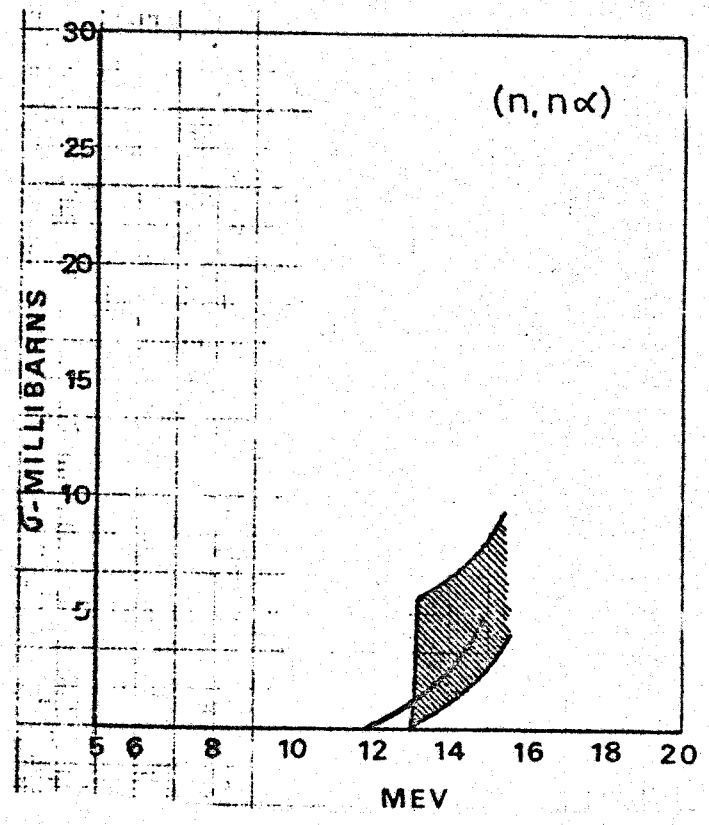
(n, nα)
σ-MILLIBARNS
30
25
20
15
10
5
5 6 8 10 12 14 16 18 20
MEV

Fig. 10

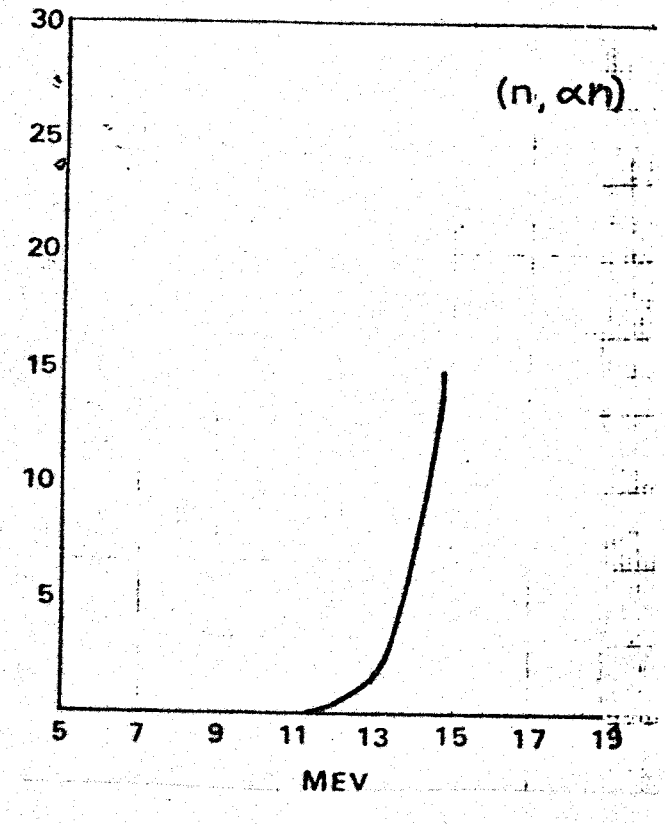
(n, αn)
30
25
20
15
10
5
5 7 9 11 13 15 17 19
MEV

Fig. 11